



Share Your Innovations through JACS Directory

Journal of Nanoscience and Technology

Visit Journal at <http://www.jacsdirectory.com/jnst>

Facile Green Synthesis of LaCe Co-Doped ZnO Nanoparticles and Their Structural, Optical and Antibacterial Properties

M. Karthikeyan¹, A. Jafar Ahamed^{1,*}, P. Vijaya Kumar²¹Post Graduate and Research Department of Chemistry, Jamal Mohamed College (Autonomous), Tiruchirappalli – 620 020, Tamil Nadu, India.²Department of Chemistry, Asan College of Arts and Science, Karur – 639 003, Tamil Nadu, India.

ARTICLE DETAILS

Article history:

Received 11 November 2018

Accepted 25 November 2018

Available online 05 December 2018

Keywords:

Zinc Oxide

Nanoparticles

Gymnema sylvestree

Antibacterial Studies

ABSTRACT

This present work describes the synthesis of LaCe co-doped zinc oxide (ZnO) nanoparticles (NPs) prepared by green method using *Gymnema sylvestree* (*G. sylvestree*) leaves as reducing as well as capping agent. Green synthesis method avoids inert gases, high pressure, laser radiation, high temperature, toxic chemicals etc. as compared to conventional method like sol-gel technique method, laser ablation method, solvothermal method, inert gas condensation method and chemical reduction method. The synthesized LaCe co-doped ZnO NPs was characterized by X-Ray diffraction (XRD), field emission scanning electron microscopy (FESEM), elemental analysis (EADX), Fourier transform infrared spectroscopy (FTIR), UV-vis spectroscopy and photoluminescence (PL). The LaCe co-doped ZnO NPs was tested against clinical pathogens such as gram positive G+ (*Staphylococcus aureus* and *Streptococcus pneumoniae*) and gram negative G- (*Klebsiella pneumoniae*, *Shigella sydentariae*, *Escherichia coli*, *Pseudomonas aeruginosa* and *Protus vulgaris*) bacterial strains using agar well diffusion method.

1. Introduction

In the past decades, nano-sized materials have attracted much attention owing to their interesting properties and potential application in many variety of fields. The properties of these materials are greatly affected by their size and shape [1, 2], which generate interest in the synthesis of semiconductor nanoparticles exhibiting different shapes, such as nanobelts and nanowires [3], nanospheres [4], nanoplates [5] and nanoflowers [6], among others.

ZnO is an n-type II-VI semiconductor having direct band gap of 3.37 eV in addition with large excitation energy 60 meV and due to this it has eminent applications such as luminescence, optoelectronics, transparent electronics, ultraviolet (UV) light emitters, piezoelectric devices etc. [7, 8]. ZnO is also suitable for UV screening applications, because it has high chemical stability, low toxicity and it is effective to inhibit pathogenic organisms [9]. In the previous studies, ZnO reveals the room temperature ferromagnetism (RTFM) when the metallic dopants like Al, Co, Mg and Mn etc., are successfully doped with ZnO NPs [10]. Sankara Reddy et al. have reported that ZnO and co-doped (Co, Ag) ZnO nanoparticles prepared by co-precipitation method without use of capping agent [11]. In the present work, LaCe co-doped ZnO NPs were synthesized by green method using *G. sylvestree* leaves extracts and their structural, optical and antibacterial properties have been investigated.

2. Experimental Methods

2.1 Green Synthesis of LaCe Co-Doped ZnO NPs

LaCe co-doped ZnO nanoparticles were prepared by green synthesis method using zinc nitrate, lanthanum nitrate and cerium nitrate as metal precursors (Zn, La and Ce respectively) and *G. sylvestree* leaves extract as reducing and capping agent. 15 g of finely chopped *G. sylvestree* leaves were weighed, then 150 mL of double distilled water was added and boiled at 80 °C for 1 h, the obtained extract was filtered using Whatman-1 filter paper and the filtrate was collected in 250 mL Erlenmeyer flask. Thereafter, 0.297 M Zn(NO₃)₂·6H₂O, 0.002 M La(NO₃)₃·6H₂O and 0.001 M Ce(NO₃)₃·6H₂O solution was added into 150 mL of *G. Sylvestree* leaves

extract and it was stirred constantly at 80 °C for 6 hours. A dull yellow colour precipitate was obtained, further the precipitate was dried at 120 °C for 6 hours. The obtained LaCe co-doped ZnO powder was annealed at 700 °C for 6 hours.

2.2 Antibacterial Assay

The antibacterial activity of the LaCe co-doped NPs was studied against gram positive (*Staphylococcus aureus* and *Streptococcus pneumoniae*) and gram negative G- (*Klebsiella pneumoniae*, *Shigella sydentariae*, *Escherichia coli*, *Pseudomonas aeruginosa* and *Protus vulgaris*) bacterial strains using well diffusion method. Petri plates were prepared with 25 mL of sterile Muller Hinton agar (MHA, Himedia) and each bacterial pathogen was individually swabbed on MHA in separate plates. The antibacterial activity was tested at a concentration of 1.5 mg/mL with the required quantity of the NPs dispersed in dimethyl sulphoxide (DMSO). The zone of inhibition levels (mm) were measured after 24 h and before this step, it was incubated overnight at 37 °C. The standard antibiotic amoxicillin was used as the positive control.

2.3 Characterization Studies

The phase purity of the synthesized NPs were determined by X-ray diffractometer (Model: X'PERT PRO PAN analytical). The morphological features of the sample were measured by Field emission scanning electron microscopy (Model: Carl Zeiss 55) with EDAX (ultras). The vibrational frequency was measured by Fourier transform infra-red spectroscopy (Perkin-Elmer). The absorption spectrum of the sample was measured on Perkin-Elmer (Lambda 35). The PL emission study of the sample was carried out using Horiba Jobin YVON spectrofluorometer (model: FLUOROMAX-4, 450W high pressure Xenon lamp as the excitation source, photomultiplier at a range 325-550 nm).

3. Results and Discussion

3.1 X-Ray Diffraction Studies

The X-ray diffraction peaks of LaCe co-doped ZnO NPs are shown in Fig. 1. The XRD peaks are located at angles (2θ) of 31.852, 34.515 and 36.302°, corresponding to the (100), (002) and (101) planes of the ZnO NPs, respectively. Similarly, other peaks found at angles (2θ) of 47.582, 56.683, 63.015, 66.48, 68.06, 69.25 and 77.06° correspond to (102), (110), (103),

*Corresponding Author: agjafar@yahoo.co.in (A. Jafar Ahamed)

(112), (201), (004) and (202) planes of ZnO NPs, respectively. All the observed diffraction peaks can be indexed to the hexagonal wurtzite structure of ZnO (space group P63mc and JCPDS 36-1451), while the existence of any crystalline secondary phase can be ruled out in the diffraction pattern [12]. The average crystalline size of the nanoparticles is calculated from X-ray line broadening using the Scherrer relation, $D = 0.9\lambda/\beta\cos\theta$, where D is the crystallite size, λ is the wavelength (1.5406 Å CuK α), θ is the Bragg diffraction angle and β is the full width at half maximum (FWHM). The average crystallite size is calculated as 42 nm for LaCe co-doped ZnO NPs.

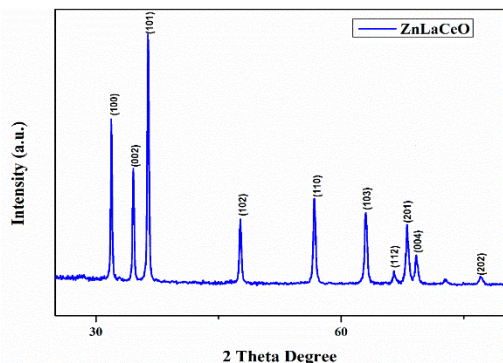


Fig. 1 XRD pattern of LaCe co-doped ZnO nanoparticles

3.2 Field Emission Scanning Electron Microscopy (FESEM) Studies

The FESEM image of the LaCe co-doped ZnO NPs is shown in Fig. 2. FESEM image clearly shows that LaCe co-doped ZnO nanoparticles form a spherical like structure. The average particle size is found to be 49 nm. This is also confirmed by the XRD results.

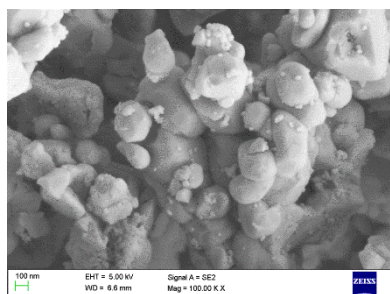


Fig. 2 FESEM image of LaCe co-doped ZnO nanoparticles

3.3 Energy Dispersive Analysis of X-Ray (EDAX) Studies

The chemical purity and elemental composition of the LaCe co-doped ZnO NPs was investigated by Energy Dispersive X-ray analysis (EDAX), is shown in Fig. 3. In the co-doped sample, LaCe composition is observed at 1.54%. The chemical composition of Zn and O are found as 83.41% and 15.05% respectively. The EDAX spectra has indicated the presence of Zn, O, La, and Ce for the synthesized NPs. The obtained NPs are made up of only these elements, which shows that the La³⁺ and Ce³⁺ ions are substituting the Zn²⁺ ions in the ZnO matrix.

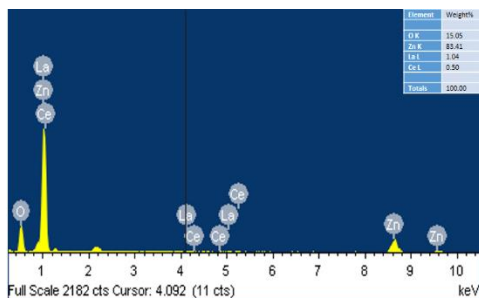


Fig. 3 EDAX spectra of LaCe co-doped ZnO nanoparticles

3.4 Fourier Transform Infrared (FTIR) Studies

The FT-IR spectra of LaCe co-doped ZnO NPs is shown in Fig. 4. The synthesized LaCe co-doped ZnO NPs was analyzed by FT-IR in the range from 400 to 4000 cm⁻¹ at room temperature. The absorption peak appeared at 3410 cm⁻¹ corresponds to the stretching vibration of the O–H

band. This absorption peak is appeared due to the O–H stretching of surface absorption of water molecules [13]. The narrow intense H–O–H bending centered at 1648 cm⁻¹. The medium intensity band 1385 cm⁻¹ is attributed to C=O symmetric stretching. The weak band observed near 873 cm⁻¹ is assigned to the metal–oxygen vibration frequency due to the changes in the micro structural features by the addition of La and Ce into Zn–O lattice [14]. The absorption bands of Zn–O stretching are exhibited in LaCe co-doped ZnO NPs are appeared at 464 cm⁻¹.

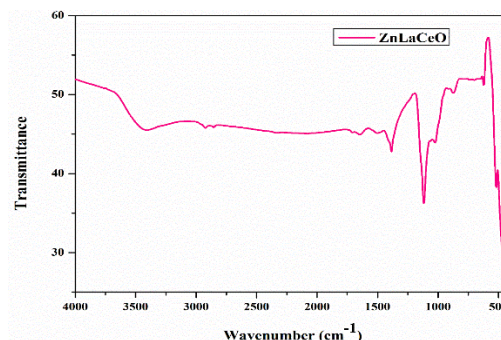


Fig. 4 FT-IR spectra of LaCe co-doped ZnO nanoparticles

3.5 UV-Vis Absorption Spectroscopy

The optical properties of LaCe co-doped ZnO NPs was investigated by UV-Vis absorption spectra, is shown in Fig. 5. From the absorption spectra, the absorption peak is found at 394 nm for LaCe co-doped ZnO NPs, which can be attributed to the photo excitation of electrons from valence band to conduction band [15].

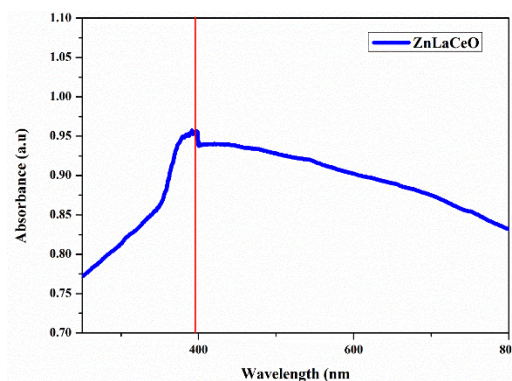


Fig. 5 Absorption spectra of LaCe co-doped ZnO nanoparticles

3.6 Photoluminescence (PL) Studies

Fig. 6 shows the photoluminescence spectra of LaCe co-doped ZnO NPs using an excitation wavelength of 350 nm. In the case of LaCe co-doped ZnO NPs, the emission wavelengths are observed at 367, 386, 395, 409, 435, 482 and 520 nm respectively. The UV emission peaks of lowest wavelength are observed at 367, 386 and 395 nm, which correspond to the near-band emission (NBE) of LaCe co-doped ZnO NPs. The two violet emissions centered at 409 and 435 nm is ascribed to an electron transition from a shallow donor level of the natural zinc interstitials to the top level of the valence band [16]. The blue green emission observed at 482 nm is ascribed to the transition between the oxygen vacancy and interstitial oxygen [17]. Finally green emission observed at 520 nm, corresponds to the singly ionized oxygen vacancies [18, 19].

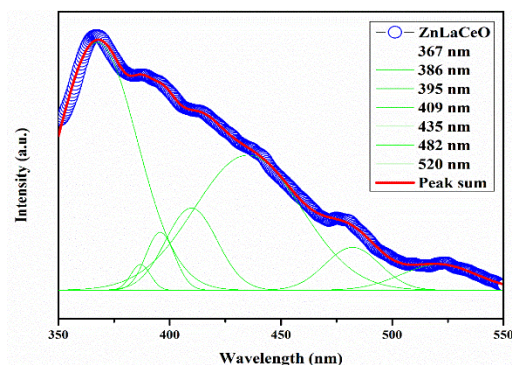


Fig. 6 PL emissions spectra of LaCe co-doped ZnO nanoparticles

Fig. 6 shows the photoluminescence spectra of LaCe co-doped ZnO NPs using an excitation wavelength of 350 nm. In the case of LaCe co-doped ZnO NPs, the emission wavelengths are observed at 367, 386, 395, 409, 435, 482 and 520 nm respectively. The UV emission peaks of lowest wavelength are observed at 367, 386 and 395 nm, which correspond to the near-band emission (NBE) of LaCe co-doped ZnO NPs. The two violet emissions centered at 409 and 435 nm is ascribed to an electron transition from a shallow donor level of the natural zinc interstitials to the top level of the valence band [16]. The blue green emission observed at 482 nm is ascribed to the transition between the oxygen vacancy and interstitial oxygen [17]. Finally green emission observed at 520 nm, corresponds to the singly ionized oxygen vacancies [18, 19].

3.7 Antibacterial Activity

The antibacterial activity was performed against a set of gram positive (G+) bacteria (*S. aureus* and *S. pneumoniae*) and gram negative (G-) (*K. pneumoniae*, *S. sydenhariae*, *E. coli*, *P. aeruginosa* and *P. vulgaris*) bacteria by agar well diffusion methods using LaCe co-doped ZnO NPs are treated with concentration 1.5 mg/mL and it is shown in Fig. 7. The zone of inhibition (ZOI) of human pathogens is shown in Fig. 8. To compare the gram positive and gram negative bacteria, the observed inhibition zone was higher in gram positive bacteria. The Zone inhibition of bacterial cells may be due to distractions of cell membrane, is mainly due to the combination of various factors such as ROS and the release of Zn^{2+} , La^{3+} and Ce^{3+} bacteria losing the viability of cell division [20-23]. This leads to killing of bacteria.



Fig. 7 The progress of antibacterial activity of LaCe co-doped ZnO NPs

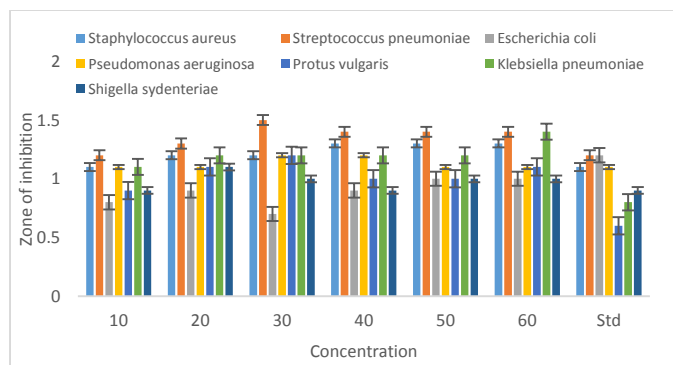


Fig. 8 The zone of inhibition formed around each disc, loaded with test samples indicated the antibacterial activity of (a) *S. aureus*, (b) *S. pneumoniae*, (c) *E. coli*, (d) *P. aeruginosa*, (e) *P. vulgaris* (f) *K. pneumoniae* and (g) *S. sydenhariae* for the LaCe co-doped ZnO NPs

4. Conclusion

The LaCe co-doped ZnO NPs synthesized by green method using *Gymnema sylvestre* leaves extract. From the X-ray diffraction study confirmed that the prepared LaCe co-doped ZnO NPs were hexagonal wurtzite structure. From the FESEM image, the morphology of nanoparticles were found spherical in shape. The elemental composition

was identified by EDAX spectra. Using the recorded FT-IR spectra, the various vibrational frequencies were assigned for the LaCe co-doped ZnO samples. The UV-Vis spectrum showed the absorption peak is found at 394 nm. PL spectra showed that doping materials altered the band emission, which is due to zinc vacancy, oxygen vacancy and surface defects. The antibacterial studies performed against a set of bacterial strains showed that the LaCe co-doped ZnO NPs possessed more antibacterial property.

References

- [1] H. Xu, W. Wang, W. Zhu, Shape evolution and size-controllable synthesis of Cu_2O octahedra and their morphology-dependent photocatalytic properties, *J. Phys. Chem. B* 110(28) (2006) 13829-13834.
- [2] M.A. El-Sayed, Some interesting properties of metals confined in time and nanometer space of different shapes, *Acc. Chem. Res.* 34(4) (2001) 257-264.
- [3] X. Wang, J. Song, Z.L. Wang, Nanowire and nanobelt arrays of zinc oxide from synthesis to properties and to novel devices, *J. Mater. Chem.* 17 (2007) 711-720.
- [4] Y.Z. Zhang, J. Chung, J. Lee, J. Myoung, S. Lim, Synthesis of ZnO nanospheres with uniform nanopores by a hydrothermal process, *J. Phys. Chem. Solids* 72 (2011) 1548-1553.
- [5] Y.C. Qiu, W. Chen, S.H. Yang, Facile hydrothermal preparation of hierarchically assembled, porous single-crystalline ZnO nanoplates and their application in dye sensitized solar cells, *J. Mater. Chem.* 20(5) (2010) 1001-1006.
- [6] Y.X. Wang, X.Y. Li, N. Wang, X. Quan, Y.Y. Chen, Controllable synthesis of ZnO nanoflowers and their morphology-dependent photocatalytic activities, *Sep. Purif. Technol.* 62 (2008) 727-732.
- [7] A. Van Dijken, E.A. Meulenkaamp, D. Vanmaekelbergh, A. Meijerink, Identification of the transition responsible for the visible emission in ZnO using quantum size effects, *J. Luminesc.* 90 (2000) 123-128.
- [8] N. Volbers, H. Zhou, C. Knies, D. Pfisterer, J. Sann, D.M. Hofmann, B.K. Meyer, Synthesis and characterization of ZnO:Co²⁺ nanoparticles, *Appl. Phys. A* 88(1) (2007) 153-155.
- [9] M. Nirmala, A. Anukalini, Characterization of undoped and Co doped ZnO nanoparticles synthesized by DC thermal plasma method, *Physica B* 406 (2011) 911-915.
- [10] S. Maensiri, P. Laokul, S. Phokha, A simple synthesis and magnetic behaviour of nanocrystalline Zn_{0.9}Co_{0.1}O powders by using Zn and Co acetates and polyvinyl pyrrolidone as precursors, *J. Magn. Magn. Mater.* 305(2) (2006) 381-387.
- [11] B. Sankara Reddy, S. Venkatramana Reddy, R.P. Vijaya Lakshmi, Structural and optical properties of Ag and Co doped ZnO nanoparticles, *AIP Conf. Proc.* 1447 (2012) 431-432.
- [12] J. Iqbal, X. Liu, H. Zhu, Z.B. Wua, Y. Zhang, D. Yu, R. Yu, Raman and highly ultraviolet red-shifted near band-edge properties of LaCe-co-doped ZnO nanoparticles, *Acta Mater.* 57 (2009) 4790-4796.
- [13] Y. Wang, X. Liao, Z. Huang, G. Yin, J. Gu, Y. Yao, Preparation and characterization of Ni doped ZnO particles via a bio assisted process, *Colloids Surf. A* 372 (2010) 165-171.
- [14] K. Raja, P.S. Ramesh, D. Geetha, Synthesis, structural and optical properties of ZnO and Ni-doped ZnO hexagonal nanorods by co-precipitation method, *Spectrochim. Acta A Mol. Biomol. Spectrosc.* 120 (2014) 19-24.
- [15] M. Liu, A. H. Kitai, P. Mascher, Point defects and luminescence centres in zinc oxide and zinc oxide doped with manganese, *J. Lumin.* 54(1) (1992) 35-42.
- [16] X.M. Fan, J.S. Lian, L. Zhao, Y. Liu, Single violet luminescence emitted from ZnO films obtained by oxidation of Zn film on quartz glass, *Appl. Sur. Sci.* 252 (2005) 420-424.
- [17] N. Varghese, L.S. Panchakarla, M. Hanapi, A. Govindaraj, C.N.R. Rao, Solvothermal synthesis of nanorods of ZnO, N-doped ZnO and CdO, *Mater. Res. Bull.* 42 (2007) 2117-2124.
- [18] N. Kumar, A. Dorfman, J. Hahn, Fabrication of optically enhanced ZnO nanorods and microrods using novel biocatalysts, *J. Nanosci. Nanotech.* 5 (2005) 1915-1918.
- [19] D.M. Bagnall, X.F. Chen, M.Y. Shen, Z. Zhu, T. Goto, T. Yao, Room temperature excitonic stimulated emission from zinc oxide epilayers grown by plasma-assisted MBE, *J. Cryst. Growth.* 184 (1998) 605-609.
- [20] N. Jones, B. Ray, K.T. Ranjit, A.C. Manna, Antibacterial activity of ZnO nanoparticle suspensions on a broad spectrum of microorganisms, *FEMS Microbiol. Lett.* 279(1) (2008) 71-76.
- [21] O. Yamamoto, Influence of particle size on the antibacterial activity of zinc oxide, *Int. J. Inorg. Mater.* 3 (2001) 643-646.
- [22] K.H. Tam, A.B. Djurišić, C.M.N. Chan, Y.Y. Xi, C.W. Tse, et al., Antibacterial activity of ZnO nanorods prepared by a hydrothermal method, *Thin Solid Films* 516 (2008) 6167-6174.
- [23] R.K. Dutta, B.P. Nenavathu, M.K. Gangishetty, A.V. Reddy, Studies on antibacterial activity of ZnO nanoparticles by ROS induced lipid peroxidation, *Colloid. Surf. B Biointerf.* 94 (2012) 143-150.